



Nanocomposite Ultrafiltration Membranes Incorporated with Zeolite and Carbon Nanotubes for Enhanced Water Separation

N. H. W. Hazmo^a, R. Naim^{*a}, A. F. Ismail^{b,c}, W.J. Lau^{b,c}, I. Wan Azelee^{b,c}, M. K. N. Ramli^{b,c}

^a Faculty of Chemical Engineering and Natural Resources, Universiti Malaysia Pahang, Lebuhraya Tun Razak, 26300 Kuantan, Pahang, Malaysia

^b Advanced Membrane Technology Research Centre (AMTEC), Universiti Teknologi Malaysia, 81310 Skudai, Johor, Malaysia

^c School of Chemical and Energy Engineering, Universiti Teknologi Malaysia, 81310 Skudai, Johor, Malaysia

PAPER INFO

Paper history:

Received 15 December 2017

Received in revised form 28 March 2018

Accepted 28 March 2018

Keywords:

Multi-Walled Carbon Nanotubes

Nanoparticles

Ultrafiltration

Zeolitic Imidazolate Framework-8

ABSTRACT

The objective of this work is to develop a new class of nanocomposite ultrafiltration (UF) membranes with excellent solute rejection rate and superior water flux using zeolitic imidazolate framework-8 (ZIF-8) and multi-walled carbon nanotubes (MWCNTs). The effect of ZIF-8 and MWCNTs loadings on the properties of polyvinylidene fluoride (PVDF)-based membrane were investigated by introducing respective nanomaterial into the polymer dope solution. Prior to filtration tests, all the membranes were characterized using several important analytical instruments, i.e., SEM-EDX and contact angle analyzer. The addition of the nanoparticles into the membrane matrix has found to increase the membrane pore size and improve its hydrophilicity compared to the pristine membrane. The separation performance of membranes was determined with respect to pure water flux and rejections against bovine serum albumin (BSA) and humic acid (HA). The experimental findings indicated that the nanocomposite membranes in general demonstrated higher permeation flux and solute rejection compared to the pristine membrane and the use of ZIF-8 was reported to be better than that of MWCNTs in preparing nanocomposite UF membranes owing to its better flux and high percentage of solute rejection.

doi: 10.5829/ije.2018.31.08b.37

1. INTRODUCTION

The preparation of nanocomposite membranes by dispersing inorganic nanoparticles in polymer matrix has attracted many interest in field of gas separation, pervaporation and ultrafiltration (UF) for over the last decades. The presence of finely dispersed nanoparticles in the membrane matrix has successfully improved the performance of membrane for separation process, especially in water and wastewater treatment field, including oil-water and protein effluent separation [1]. The main concerns in membrane filtration are flux decline and rejection reduction. It has been reported that the factors affecting the membrane separation process were solution chemistry (pH, ionic strength, and water hardness); the properties of membrane (pore size, water permeability, charge, hydrophobicity/philicity); and filtration process condition (concentration, charge and

humic and non-humic fractions) and operational conditions [2].

Polyvinylidene fluoride (PVDF) is a common material for UF membrane preparation due to its excellent chemical resistance, great mechanical properties and thermal stability [3]. However, PVDF membrane is prone to fouling due to its inherent hydrophobicity. Many works have been reported to increase the hydrophilicity of PVDF membrane by the chemical modification methods but the main polymer molecules would change and its advantages might as well be reduced. Compared to chemical modification, physical modification is more preferable for PVDF membranes modification, for enhancing the membrane hydrophilicity, permeability, rejection and mechanical strength [4]. Utilizing inorganic additive within membrane is relatively simple approach since it only focused on blending between with two phases during the

*Corresponding Author Email: rosnawati@ump.edu.my (R. Naim)

preparation of membrane. Moreover, inorganic materials such as zinc oxide (ZnO), titanium oxide (TiO₂), alumina (Al₂O₃), and graphene-based particles are easy to mix with polymer resulting in excellent properties and stable performances [5].

The recent trend explored the viability and applicability of using nanostructural metal-organic frameworks (MOFs) for new type of nanocomposite membrane synthesis. Zeolites were successfully utilized in chemical industry for over 35 years and zeolitic imidazolate frameworks 8 (ZIF-8) was found to have superior adaptability in polymer matrix [6]. It is because of the high regularity, well-defined pore structure and excellent stability, zeolites have been introduced in membrane separations. Besides, two immiscible high performance polymer blends (PBI and 6FDA) were compatibilised using ZIF-8 as its nano-sized particles featuring a uniform domain pore size in the membrane matrix [7]. Additionally, ZIF-8 also possesses the excellent solvent resistance and thermal and chemical stability [8]. Another special ability of ZIF-8 is the controllability of its particle size. The size of particle of produced ZIF-8 can be reached up to 1 nm by simply controlling its synthesis parameters or additive concentrations. It is very important to control its crystal size factor during the fabrication of asymmetric MMM, to ensure that the fillers are small enough to be able to reside among the dense, thin selective layer [9].

Multi-walled carbon nanotubes (MWCNT) is also one of the common materials used in UF membrane fabrication. It has high specific surface area, easy functionalization, good chemical stability and thermal reductant which are very useful in separation process [10]. Research also found that the viscosity and thermal conductivity of CNT can be enhanced with temperature rise and nanoparticle concentration [11]. It also has been reported that the nano-sized CNTs could lead to the increase of efficient filtration area and permeability of the composite membranes [12] as well as improved hydrophilicity and rejection [13,14]. Besides, the physical properties of the membranes such as surface properties, pore structure and tensile strength, were altered by the presence of CNTs even at very low loadings, resulting in higher antifouling and organic matter rejection. MWCNTs have promising properties for water treatment, both in mitigating membrane fouling through the inhibition of bacterial growth, and in improving the separation selectivity due to their narrow pore size distribution [15].

Furthermore, with the addition of hydrophilic polymers such as polyethylene glycol (PEG) and polyvinylpyrrolidone (PVP), the morphology and performance of membrane have been reportedly improved leading to increased high water flux [16]. It was found that addition of PVP could increase the membrane hydrophilicity due to the residue trapped in

the membrane matrix [17]. In this work, PVP was used as pore former agent to enhance the membrane porosity. Then, the properties of nanocomposite membranes will be studied by varying the content of ZIF-8 and MWCNT in the PVDF dope solution. The synthesized membranes will be used in the separation of bovine serum albumin (BSA) and humic acid (HA).

2. EXPERIMENTAL

2.1. Materials The polymeric membrane material, polyvinylidene fluoride (PVDF), the solvent, N,N-dimethylacetamide (DMAc) were supplied by Merck Malaysia. The multi-walled carbon nanotubes (MWCNTs) with >98% carbon; 10nm x 1 nm x 4.5nm (O.D x I.D x L) and the polyvinylpyrrolidone (PVP K-30) with average molecular weight of 30,000Da were purchased from Sigma-Aldrich. The chemicals used for synthesis of ZIF-8 were zinc nitrate hexahydrate (Zn(NO₃)₂·6H₂O), triethylamine (TEA) and 2-Methylimidazole (2-MeIM) were supplied by Sigma. Bovine serum albumin (BSA) and humic acid (HA) purchased from Thermo Fischer Scientific Inc. were used as solution model for the solute rejection tests.

2.2. Synthesis of ZIF-8 The ZIF-8 was synthesized by referring the procedure reported in literature [18] with ratio of Zn(NO₃)₂:2-MeIM:H₂O 1:6:500. Firstly, metal salt solution was prepared by dissolving 4g zinc nitrate hexahydrate into 24.22g of deionized water. Then, the ligand solution was prepared by weighing 6.624g of 2-MeIM and dissolved in 96.90g of deionized water, followed by adding 6.0ml of TEA into the mixture. After that, the metal salt solution was added into the ligand solution and stirred vigorously for 30 minutes. The solution was then centrifuged for 15 minutes and thoroughly washed using deionized water for several times to completely remove the excess reactants. Then, the product obtained was dried at 60°C for 12 h. Next, the product was ground into fine particles before dried in oven at 110°C for at least 12 h for further removal of trapped water/residuals in the pores.

2.3. Preparation of Membrane The flat sheet nanocomposite membranes were prepared using phase inversion method. The casting solution was prepared by blending 15 wt.% PVDF, and 1 wt.% PVP with 84 wt.% DMAc. Nanoparticles with specific loading was then added into the dope solution as shown in Table 1. The percentage of filler loading can be calculated as follows:

$$\text{Filler loading (\%)} = \frac{M_f(g)}{M_f(g) + M_s(g)} \times 100\% \quad (1)$$

where M_f is mass of fillers and M_s is mass of solids.

TABLE 1. Composition of nanoparticles in casting solution

Type of sample	No. sample	Nanoparticles, wt%
PVDF	P0	0.00
	Z1	0.10
PVDF + ZIF-8	Z2	0.30
	Z3	0.50
	M1	0.10
PVDF + MWCNT	M2	0.30
	M3	0.50

Initially, the PVDF pellet and nanoparticles (ZIF-8) were weighed and dried in oven at 60°C for at least 12 h to remove trapped water in the pores. Then, the additive PVP was dissolved in DMAc solvent followed by the addition of ZIF-8. The solution was then sonicated for 1 h to fully disperse the nanoparticles in the solvent. Next, the polymer was added into the solution and stirred at 60°C for 20 h. The casting solution was then degassed for 30 minutes to remove the trapped bubbles.

For MWCNT/PVDF membrane, the composition and procedure used was the same as ZIF-8/PVDF membrane as stated in Table 1. The dope solution was manually casted on the glass plate using glass rod, and immediately immersed in the coagulation bath of water. The formed membrane was peeled off from the plate and immersed into distilled water for complete removal of solvent. The membranes were stored in distilled water for further use.

2. 4. Characterizations The scanning electron microscopy (SEM) (Hitachi TM3030Plus, Japan) was used to examine the cross-sectional structures of the membranes. All membranes were prepared by fractured with liquid nitrogen and coated with a thin layer of gold. The membranes morphology was observed using SEM equipped with an energy dispersive X-ray spectrometer (EDX) (Oxford Instruments SwiftED3000) for compositional analysis. The contact angle (θ) analysis was used to determine the wettability of membrane by measuring the angle between water and membrane surface using goniometer (Kruss Gambult, Germany). A 3 μ l of distilled water was dropped on top surface of membrane, and after 30s the contact angles were measured to evaluate the hydrophilicity of the membrane. The average value of three contact angle was calculated for each sample at various position. Transmission electron microscope (TEM) (TECNAI G2 20 Twin) was employed to examine the macrostructures of synthesized ZIF-8. Prior to imaging, the sample was prepared by dispersing ZIF-8 powder into methanol with the aid of ultrasound. Then, a drop of the sample was transferred to 400 mesh carbon-coated copper grid and dried, before operated at 200 kV.

2. 5. Performance of Membrane

The performances of all membranes were evaluated by pure water permeability flux and solute rejection test. Both tests were measured by ultrafiltration (UF) experimental equipment with the membrane surface area of 42 cm². The pure water permeability (PWP) test was carried out using reverse osmosis water as the feed. The experiment was conducted at room temperature, with pre-compaction pressure was set at 1.5 bar for 30 min. Then, the operating pressure was adjusted to 1.0 bar for 15 min to reach steady state. The permeates were read periodically every 10 min and the time taken for volume permeate, Q=10ml was measured. The permeation flux was calculated using Equation (2):

$$J_1 = \frac{V}{A \times \Delta t} \quad (2)$$

where V is the total volume of permeated pure water during the time interval (Δt) and A is the membrane area.

On the other hand, the solute rejection tests were performed using BSA and HA solution as the feed. The BSA and HA solution were prepared with initial concentration of 500ppm. The procedures and condition were same as pure water permeability test. The time taken for the permeate flux Q=10ml was recorded for every t=10min. The percentage of solute rejection, R(%) for both solutions were determined using Equations (2) and (3), respectively:

$$R = (1 - \frac{C_p}{C_f}) \times 100\% \quad (3)$$

where C_f and C_p are the solution concentrations of feed and permeate, respectively. The concentration of all BSA and HA permeates and feed were measured using the HACH DR5000UV-Vis Spectrophotometer at a wavelength of 254 nm and 280 nm, respectively. The calculated fluxes and rejection rate are tabulated in Table 2.

3. RESULTS AND DISCUSSION

3. 1. Characterization of ZIF-8 Figure 1 presents the TEM images of the synthesized ZIF-8 at different magnifications. It can be seen that the prepared ZIF-8 possessed hexagonal morphology with the range of particle size of ZIF-8 estimated from TEM images was 80 to 130 nm. The variety in sizes of the produced ZIF-8 as mentioned before, can be reach up to 1 nm by simply control its synthesis parameters or additive concentrations. Moreover, this result is in agreement with the previous findings in which the size of the synthesized ZIF-8 was in the range of 40 to 80 nm [19], 50 nm [20] and 147.26 \pm 7.05 nm [21].

3. 2. Characterizations of Membrane The SEM analysis was performed to examine the membrane

morphology between the pure PVDF membrane with the nanocomposite membranes. Figure 2 shows the SEM images of the surface and cross-section morphologies for pristine, ZIF-8/PVDF and MWCNT/PVDF membranes. Obviously, a finely dispersed nodular structure packed by the spherical globules on the membrane layer can be observed on top surface of Z3 in Figure 2(a). This phenomenon may result from the integration of ZIF-8 and polymer structure. Meanwhile, M1 displayed a better surface morphology than P0 with higher number of pores and large pore sizes. This is may due to the oxygen content in MWCNT that facilitated the diffusion rate during the preparation process.

From the observation, the morphologies of the nanocomposite membranes have been improved upon addition of nanoparticles, compared to pristine PVDF membrane. It can be seen that the cross-section morphology of the prepared membranes Z1, Z2, Z3, and M1 exhibited narrow finger-like structures while, larger macro-voids can be observed for M2 and M3 compared to pristine membrane.

Furthermore, the membranes presented the asymmetric structure with a selective thin microporous upper layer on a large voids or finger-like cavities due to the high mutual diffusivity of solvent and water [22]. The blend membranes demonstrated a strong change in the morphology.

TABLE 2. EDX quantitative analysis of all membranes

Sample	C	F	Zn	Pt
P0	37.97	56.84	-	5.19
Z1	39.89	55.03	0.11	4.97
Z2	40.47	54.43	0.28	4.82
Z3	41.06	53.40	0.50	5.01

Sample	C	F	O	Al	Pt
M1	40.54	52.25	3.21	0.001	4.00
M2	41.13	51.38	3.69	0.006	3.80
M3	41.96	50.40	4.18	0.011	3.45

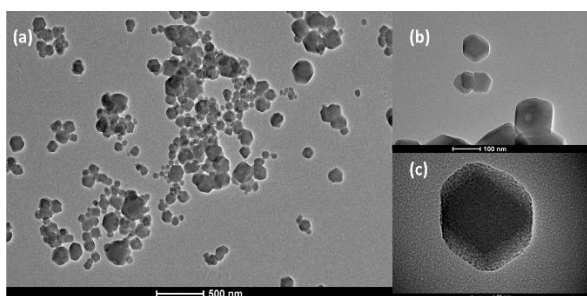


Figure 1. TEM images for synthesized ZIF-8 at different magnifications; (a) images taken at scale of 500 nm, (b) image taken at 100 nm, and (c) image taken at 20 nm

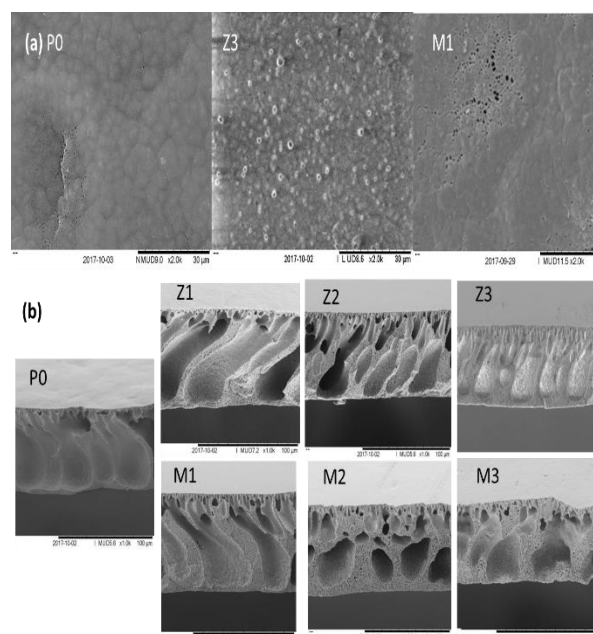


Figure 2. SEM images of (a) surface of P0, Z3 and M1; (b) cross section of all membranes with different compositions

The pore sizes for all blend membrane were completely different from pristine membrane. After addition of zeolite materials, the cross-section became a little denser. When 0.1wt% ZIF-8 content was added, the typical finger-like structures (Figure 2(b):Z1) can be observed. The pristine membrane revealed larger finger-like structures but it grew narrower and sponger as ZIF-8 content increased. Besides, the pore size tended to decrease accordingly, making the structure denser. Z2 started to form smaller and narrower finger-like structures compared to pristine membrane and Z3 showed more compact structure with lesser finger-like as the ZIF-8 content increased. This might related to the increased in viscosity of the casting solution which lead to the slower phase separation process, resulted in smaller pore size and denser structure.

The SEM images of MWCNT/PVDF membranes revealed a more porous structure than the plain membrane. It formed narrower finger-like structure for M1, but the pore size kept increasing with increasing MWCNT contents. The pore size of the macro-voids M2 and M3 were observed to increase and instability structures was formed. During the phase inversion, the diffusion rate between solvent and water was accelerated by MWCNTs. Additionally, MWCNT possessed oxygen-containing functional groups that made it typical hydrophilic materials and accelerated the mass transformation between the solvent and non-solvent [23]. Therefore, larger pore channels were formed due to the rapid mass transformation. This may facilitates the membrane permeability which reflects to the increase in membrane pores size. Relatively, as contents of the

nanoparticles increased, the membrane pore sizes will start to increase as well, which may have a relation with improved water permeability; $M3 > M2 > M1$. The M3 contained largest macro-voids and more porous, resulted in highest water flux as the water molecule can pass through the membrane pores easily.

3. 3. EDX analysis Table 2 shows the quantitative analysis of elements present in the membrane. The detection of Pt element was due to the coating material used prior to SEM analysis. The EDX analysis of Z3 in Figure 3(a) showed the presence of Zn element indicating the existence of ZIF-8 particles in the membrane. Furthermore, the Zn element were well-distributed throughout the membrane matrix. This can be proven by the value of Zn loading present in the membrane was 0.501 wt% which has good agreement with the calculated filler loading 0.499 wt%. This indicated that the ZIF-8 nanoparticles were uniformly dispersed during the fabrication process. The ZIF-8 loading for Z1 and Z2 in Table 2 also in good term with the calculated filler loading which was 0.0999 wt% and 0.2991 wt%, respectively.

All the elements present in the membrane matrix are tabulated in Table 2. Carbon and fluorine were originally from the PVDF polymer. The new elemental zinc, oxygen and aluminium found in the membrane matrix were from ZIF-8 and MWCNT, respectively. In this work, MWCNT is mainly consisted of element C, O, H with >98% carbon basis. Another 2% element that may be found in the CNT was aluminium (Al) from Al_2O_3 electrode substrate.

Figure 3(b) shows the carbon loading increased with addition of MWCNT indicated that it has fully dissolved in the polymer matrix and the oxygen element confirmed the presence of carbon nanotubes in the membrane. Besides, the data on 2% Al loading (Table 2) found in the membrane matrix also compatible with the calculated loading which are 0.002% for M1, 0.006% for M2 and 0.01% for M3.

This confirms the MWCNT has fully dispersed and well-distributed throughout the membrane matrix.

Table 3 shows the average of contact angle values for all the membranes. As expected, the addition of nanoparticles has enhanced the pore size of the membrane. Generally, the small value of contact angle corresponds to more hydrophilic properties. Compared to the pristine PVDF membrane, the nanocomposite membranes tend to have larger pore size and more porous upon the increased contents of nanoparticles as shown in Figure 2. This showed that the hydrophilicity of the membrane has been improved with addition of ZIF-8 and MWCNT.

The overall contact angle values decreased as the concentration of nanoparticles increased. Pristine PVDF membrane has high contact angle of 77.81° while membranes with larger pores tend to have lower contact angle. ZIF-8/PVDF membrane showed increment in hydrophilicity, started with contact angle of 66.51° for Z1. The values decreased with Z2 (64.41°) followed by Z3 (58.23°). For MWCNT/PVDF membrane, the membrane hydrophilicity has been improved rapidly, especially M3 with contact angle of 53.59° which suggest the positive effect of MWCNT on membrane hydrophilicity. As a result, this may play a favourable role in elevating the water flux of nanocomposite membranes.

3. 4. Performances of Membrane The membrane hydrophilicity plays a great influence on its antifouling property and filtration performance. Figure 4 shows the effect of nanoparticles on the permeability of membrane. Compared to the pristine membrane, it was found that when the content of ZIF-8 nanoparticles was increased from 0.1 to 0.5 wt.%, the pure water flux of the membrane increased correspondingly.

Since the pristine membrane revealed smaller pore size and less macro-voids (Figure 2), the greater transport resistance across the membranes has resulted in low water permeate flux. However, a decline in water flux has been observed upon addition of 0.3 wt.% and 0.5 wt.% of ZIF-8 in the casting solution due to the decrease in pore size and more compact structure.

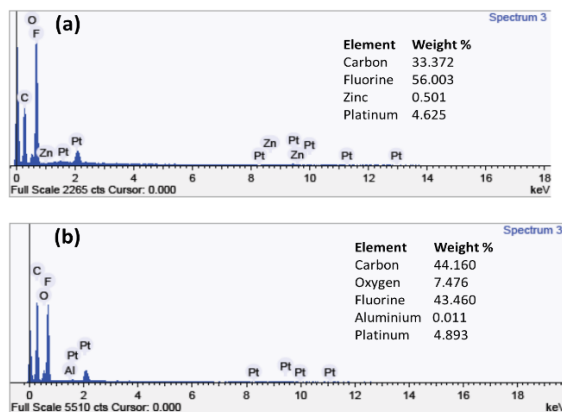


Figure 3. EDX analysis of cross sectional morphology of (a) Z3 and (b) M3

TABLE 3. Contact angle value of all membranes

Type	Average values of contact angle	Standard Deviation
P0	77.81	±0.61
Z1	58.23	±0.90
Z2	64.35	±1.03
Z3	66.51	±1.04
M1	60.66	±1.39
M2	56.26	±0.68
M3	53.59	±0.71

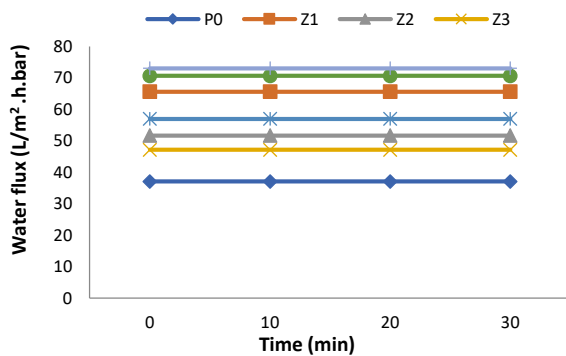


Figure 4. Water permeability flux of all membranes

The same trend can be found for MWCNT as well. The pure water flux increased with addition of MWCNT in the casting solution. Further increase in MWCNT concentration resulted in higher permeability of the membrane due to increased macro-void structures. Considering the result, the improvement in permeability of M2 and M3 might be caused by oxygen-functional group in MWCNT which facilitated the membrane hydrophilicity (Table 3). Moreover, less oxygen-content may limited the improvement in membrane porosity, mean pore size and membrane hydrophilicity. Consequentially, MWCNT/PVDF membrane have higher membrane permeability compared to ZIF-8/PVDF and pristine PVDF membranes.

Two types of solute solutions (BSA and HA) were applied to explore the UF performance under normal operating pressure of 1 bar at room temperature. The filtration performance are presented in Figures 5 and 6. Based on Figure 5(a), it was found that the ZIF-8/PVDF membrane showed an increase in permeate flux of BSA solution compared to the pristine membrane. Obviously, Z3 has higher flux with $28.76 \text{ L/m}^2 \cdot \text{h} \cdot \text{bar}$ compared to P0 which was $23.8 \text{ L/m}^2 \cdot \text{h} \cdot \text{bar}$ but lower than M2 and M3 due to difference in porosity and less macro-voids structures. The greater flux achieved by M2 and M3 probably due to relatively large pore sizes. However, the permeate fluxes of all membranes started to decrease as the filtration time increased. The permeate flux for Z2, Z3 and M1 in BSA solution started to show a decrease value at the filtration time, $t=30 \text{ min}$, while M2 and M3 declined after $t=10 \text{ min}$.

The same trend also applied for HA solution. The permeate fluxes for Z1, Z2 and Z3 decreased at $t=30 \text{ min}$ while P0 declined after $t=20 \text{ min}$. The difference in molecular weight of humic acid solute which varies from 20-500 KDa, might affects the flux and rejection differently for each membrane [24]. Membrane with larger pore size tend to have higher permeate flux as the small solutes in HA solution can pass through the macro-voids easily.

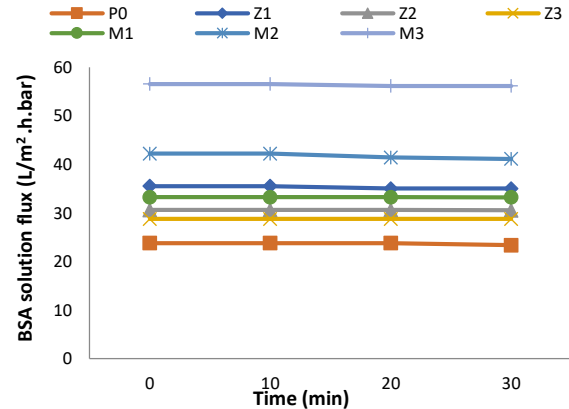


Figure 5(a). Membrane permeate fluxes for BSA solution

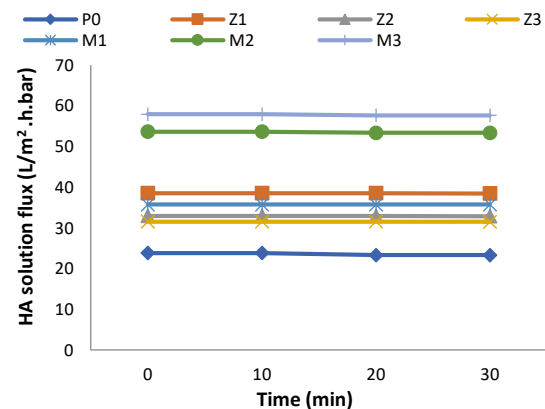


Figure 5(b). Membrane permeate fluxes for HA solution

M2 and M3 have higher flux compared to other nanocomposite membrane and pristine membrane, although the fluxes kept decreased as the time passed. M2 and M3 deteriorated after $t=10 \text{ min}$, while other membrane started to decrease at $t=30 \text{ min}$.

Figure 6 shows the percentage of rejection for BSA and HA solute. As could be seen from Figure 6(a), Z3 has highest rejection percentage of BSA solution compared to other membranes. The nanocomposite membranes demonstrated an increase in solute rejection as nanoparticles contents increased with 92.31% of Z3, 90.75% for Z2, 89.89% for M1, 87.44% for Z1, 83.72% for M2 and 78.29% for M3. As discussed earlier, the denser structure and smaller pore size of Z1 and Z2 acted favorably towards HA solute by preventing the solutes from entering the pore on top surface and passing the pore length to minimize the possibility of pore blockage and/or pore narrowing, thus increase the rejection rate.

Commonly, CNTs exhibit the capability to remove albumin as a type of adsorbent [25]. This can be seen in Figure 6(a), M1 and M2 have higher percentage of BSA solute rejection compared to pristine membrane (82.52%).

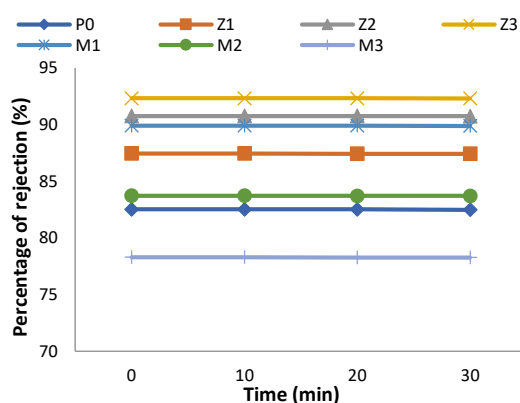


Figure 6(a). Percentage of rejection of BSA solute for all samples

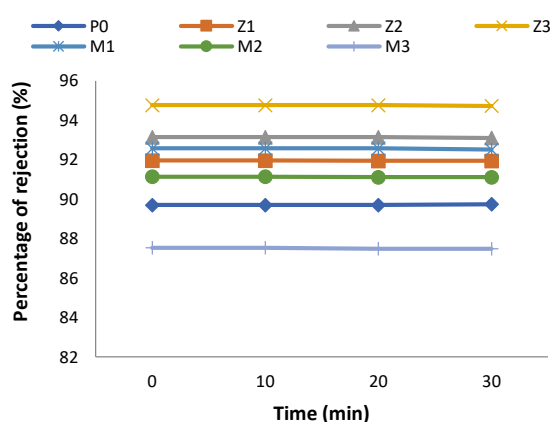


Figure 6(b) Percentage of rejection of HA solute for all samples

Compared to ZIF-8/PVDF membranes, MWCNT/PVDF membrane showed a reduction in BSA solute rejection as its concentration increased, due its macro-porous structure that might help BSA solutes escaped the pores easily. However, the rejection rate of all membranes has deteriorated over filtration time. Z2, Z3 and M1 has reduction in solute rejection at $t=30$ min, while M2 and M3 decreased after $t=10$ min.

The high separation of HA solute can be explained by the difference in pore size of membrane and size of HA. From Figure 6(b), Z3 exhibited highest HA solute rejection compared to other membranes with 94.77%, followed by Z2 with 93.14% rejection, 92.57% for M1, 91.96% for Z1, 91.11% for M2 and lastly M3 with 87.53%. Overall, all the nanocomposite membrane presented higher percentage of HA solute rejection than the pristine membrane (89.70%). Unfortunately, the solute rejection rate of all membranes started to decline over the filtration time; rejection of M3 rapidly reduced after $t=10$ min. This is probably due to large macro-voids which trapped the solute and deteriorated the filtration performance.

4. CONCLUSION

In this study, flat sheet PVDF membranes with different properties have been prepared by incorporating ZIF-8 and MWCNT. The ZIF-8 was successfully synthesized and confirmed by literature. The ZIF-8/PVDF membrane with 0.5 wt.% concentration was found to has the highest percentage of solute rejection for both BSA (>92%) and HA (>94%) solution. The experimental results showed that with addition of nanoparticles in membrane matrix, an improvement in the hydrophilicity of membrane can be achieved as well as membrane permeability and rejection rate. As the concentration of nanoparticles increased, the membrane structure also increased. For ZIF-8/PVDF membrane, the increased in concentration facilitated the water flux and rejection rate for both BSA and HA solution. Meanwhile, water flux of MWCNT/PVDF increased rapidly although the rejection rate of the membranes started to reduce when the concentration increased. In the nutshell, the addition of nanoparticles has enhanced the membrane permeability and filtration performance in the water separation process.

5. ACKNOWLEDGEMENT

The authors would like to express sincere gratitude to Ministry of Higher Education and Universiti Teknologi Malaysia for the financial support through Higher Institution Centre of Excellence (HiCoE) Grant Vot R.J090301.7809.4J181. This work also financially supported by the Universiti Malaysia Pahang under the research grant RDU170348.

6. REFERENCES

1. Y. Zhao, Z. Xu, M. Shan, C. Min, B. Zhou, Y. Li, B. Li, L. Liu, X. Qian, "Effect of Graphite Oxide And Multi-Walled Carbon Nanotubes on The Microstructure and Performance of PVDF Membranes", *Separation and Purification Technology*, Vol. 103 (2013) 78–83.
2. J. Cho, G. Amy, J. Pellegrino, "Membrane Filtration of Natural Organic Matter; Factors and Mechanisms Affecting Rejection and Flux Decline With Charged Ultrafiltration (UF) Membrane", *Journal of Membrane Science*. Vol. 164 (2000) 89–110.
3. J. Li, X. Liu, J. Lu, Y. Wang, G. Li, F. Zhao, "Anti-bacterial properties of ultrafiltration membrane modified by graphene oxide with nano-silver particles", *Journal of Colloid and Interface Science*, Vol. 484 (2016) 107–115.
4. J. Ma, Y. Zhao, Z. Xu, C. Min, B. Zhou, Y. Li, B. Li, J. Niu, "Role of oxygen-containing groups on MWCNTs in enhanced separation and permeability performance for PVDF hybrid ultrafiltration membranes", *Desalination*, Vol. 320 (2013) 1–9.
5. R. Zhang, Y. Liu, M. He, Y. Su, X. Zhao, M. Elimelech, Z. Jiang, "Antifouling Membranes for Sustainable Water Purification: Strategies and Mechanisms", *Chemical Society Reviews*, Vol. 45 (2016) 5888–5924.

6. H. Esfandian, M. Parvini, B.Khoshandam, A. Samadi-Maybodi, "Removal of Diazinon from Aqueous Solutions in Batch Systems Using Cu-modified Sodalite Zeolite: an Application of Response Surface Methodology", *International Journal of Engineering, Transaction B: Applications*, Vol. 28, No.11, (2015), 1552-1563.
7. N. P. Panapitiya, S.N. Wijenayake, Y. Huang, D. Bushdiecker, D. Nguyen, C. Ratanawanate, G.J. Kalaw, C.J. Gilpin, I.H. Musselman, K.J. Balkus, J.P. Ferraris, "Stabilization of Immiscible Polymer Blends Using Structure Directing Metal Organic Frameworks (MOFs)", *Polymer*, Vol. 55 (2014) 2028-2034.
8. D. Ge, H. K.Lee, "Water stability of zeolite imidazolate framework 8 and application to porous membrane-protected micro-solid-phase extraction of polycyclic aromatic hydrocarbons from environmental water samples", *Journal of Chromatography A*, Vol. 1218 (2011) 8490– 8495
9. S. Hwang, W. Chi, S. J. Lee, S. HyukIm, J. H. Kim, J-soo Kim, "Hollow ZIF-8 nanoparticles improve the permeability of mixed matrix membranes for CO₂/CH₄ gas separation", *Journal of Membrane Science*, Vol. 480 (2015) 11–19
10. A. Chaboki, S. A. Sadrnejad, M. Yahyaieii. "Stress Transfer Modelling in Cnt Reinforced Composites Using Continuum Mechanics", *International Journal of Engineering, Transaction B: Applications*, Vol. 21, No.3, (2008), 227-234.
11. M. Thakur, D. Gangacharyulub, G. Singh, "An Experimental Study on Thermophysical Properties of Multiwalled Carbon Nanotubes", *International Journal of Engineering Transactions B: Applications*, Vol. 30, No. 8, (A2017) 1223-1230.
12. H. Q. Wu, B.B. Tang, P.Y. Wu, "Novel Ultrafiltration Membranes Prepared from a Multi-Walled Carbon nanotubes/Polymer Composite", *Journal of Membrane Science*, Vol. 362 (2010) 374–383.
13. J.-H. Choi, J. Jegal, W.-N. Kim, "Fabrication and characterization of multi-walled carbon nanotubes/polymer blend membranes", *Journal of Membrane Science*, Vol. 284 (2006) 406–415.
14. S. Majeed, D. Fierro, K. Buhr, J. Wind, B. Du, A. Boschetti-De-Fierro, V. Abetz, "Multi-walled Carbon Nanotubes (MWCNTs) Mixed Polyacrylonitrile (PAN) Ultrafiltration Membranes", *Journal of Membrane Science*, Vol. 403 (2012) 101–109.
15. T-Y. Liu, Y. Tong, Z-H. Liu, H-H. Lin, Y-K. Lin, B. V. Bruggen, X-L. Wanga, "Extracellular Polymeric Substances Removal of Dual-Layer (PES/PVDF) Hollow Fiber UF Membrane Comprising Multi-Walled Carbon Nanotubes For Preventing RO Biofouling", *Separation and Purification Technology*, Vol. 148 (2015) 57–67.
16. J. Xu, Z-L. Xu, "Poly(vinyl chloride) (PVC) hollow fiber ultrafiltration membranes prepared from PVC/additives/solvent", *Journal of Membrane Science*, Vol. 208 (2002) 203–212.
17. C. Tang, W. Chen, W. Chen, Q. Fua, Z. Du, Y. Ye, M. Onishi, N. Abe, "Effect of Solution Extrusion Rate on Morphology and Performance of Polyvinylidene Fluoride Hollow Fiber Membranes Using Polyvinyl Pyrrolidone as an Additive", *Chinese Journal of Polymer Science*, Vol. 28, No. 4, (2010), 527–535.
18. N. A. H. M. Nordin, A. F. Ismail, A. Mustafa, R. S. Muralia, T. Matsuura, "Utilizing low ZIF-8 loading for an asymmetric PSf/ZIF-8 mixed matrix membrane for CO₂/CH₄ separation", *RSC Advances*, Vol.5 2015, 30206-30215.
19. J. Wang, Y. Wang, Y. Zhang, A. Uliana, J. Zhu, J. Liu, and B. V. Bruggen, "Zeolitic Imidazolate Framework/Graphene Oxide Hybrid Nanosheets Functionalized Thin Film Nanocomposite Membrane for Enhanced Antimicrobial Performance", *ACS Applied Material Interfaces* (2016), 8, 25508–25519.
20. L. Dong, M. Chen, J. Li, D. Shi, W. Dong, X. Li, Y. Bai, "Metal-organic framework-graphene oxide composites: A Facile Method to Highly Improve The CO₂ Separation Performance of Mixed Matrix Membranes", *Journal of Membrane Science*, Vol.520 (2016) 801–811.
21. E. M. Mahdi, J-C. Tan, "Dynamic Molecular Interactions Between Polyurethane and ZIF-8 in a polymer-MOF nanocomposite: Microstructural, Thermo-mechanical and Viscoelastic Effects", *Polymer*, Vol.97 (2016) 31-43.
22. A. Bottino, G. Capannelli, A. Comite, "Preparation and characterization of Novel Porous PVDF–ZrO₂ Composite Membranes", *Desalination*, Vol. 146 (2002) 35–40.
23. Z. Yu, G. Zeng, Y. Pan, L. Lv, H. Min, L. Zhang, Y. He, "Effect of Functionalized Multi-Walled Carbon Nanotubes on The Microstructure And Performances of PVDF Membranes", *RSC Advances*, Vol. 5, (2015) 75998–76006 DOI: 10.1039/C5RA12819F.
24. N. A. A. Hamid, A. F. Ismail, T. Mastura, A. W. Zularisam, W. J. Lau, E. Yuliwati, M.S. Abdullah, "Morphology and Separation Performance Study of Polysulfone/titanium dioxide (PSF/TiO₂) Ultrafiltration Membranes for Humic Acid Removal", *Desalination*, Vol. 273 (2011) 85-92.
25. A. Alpatova, M. Meshref, Kerry N. McPhedran, M. Gamal El-Din, "Composite polyvinylidene fluoride (PVDF) membrane impregnated with Fe₂O₃ nanoparticles and multiwalled carbon nanotubes for catalytic degradation of organic contaminants", *Journal of Membrane Science*, Vol.490 (2015) 227–235.

Nanocomposite Ultrafiltration Membranes Incorporated with Zeolite and Carbon Nanotubes For Enhanced Water Separation

N. H. W. Hazmo^a, R. Naim^a, A. F. Ismail^{b,c}, W.J. Lau^{b,c}, I. Wan Azelee^{b,c}, M. K. N. Ramli^{b,c}

^a Faculty of Chemical Engineering and Natural Resources, Universiti Malaysia Pahang, Lebuhraya Tun Razak, 26300 Kuantan, Pahang, Malaysia

^b Advanced Membrane Technology Research Centre (AMTEC), Universiti Teknologi Malaysia, 81310 Skudai, Johor, Malaysia

^c School of Chemical and Energy Engineering, Universiti Teknologi Malaysia, 81310 Skudai, Johor, Malaysia

PAPER INFO

چکیده

Paper history:

Received 15 December 2017

Received in revised form 28 March 2018

Accepted 28 March 2018

Keywords:

Multi-Walled Carbon Nanotubes

Nanoparticles

Ultrafiltration

Zeolitic Imidazolate Framework-8

هدف از انجام این پژوهش، توسعه یک نوع جدید از غشاهای اولترافیلتراسیون (UF) نانوکامپوزیتی است که دارای میزان پسزدگی مطلوب املاح و نیز شار بالای آب میباشد. این غشاها با استفاده از پایه ایمیدازول زئولیتی (ZIF-8) و نانولوله های کربنی چنددیواره (MWCNTs) تهیه شدند. تأثیر بارگذاری ZIF-8 و MWCNTs بر خصوصیات غشای پلی وینیل دی فلوراید با افزودن نانومواد مربوطه به محلول پلیمری مورد بررسی قرار گرفت. قبل از آزمایش های فیلتراسیون، ویژگیهای تمام غشاهای ساخته شده با استفاده از چندین تکنیک، مانند SEM-EDX و آنالیز زاویه تماس، مشخص شد. افزودن نانو ذرات به ماتریس غشایی، سبب افزایش اندازه روزنه های غشا شد و آبدوستی آن را نسبت به غشاء اولیه بهبود بخشید. عملکرد غشاهای ساخته شده در مورد آلومین سرم گاوی و اسید هیومیک با توجه به شار آب خالص و املاح برگشتی تعیین شد. یافته های آزمایشی نشان داد که غشاهای نانوکامپوزیتی به طور کلی دارای شار نفوذی و برگشتی بیشتری نسبت به غشاء اولیه است و استفاده از ZIF-8 در تهیه غشاهای اولترافیلتراسیون نانوکامپوزیتی به دلیل شار مطلوب و درصد بالای املاح برگشتی، بهتر از MWCNTs است.

doi: 10.5829/ije.2018.31.08b.37